Journal of Applied Polymer Science

Behavior of UV-Cured Print Inks on LDPE and PBAT/TPS Blend Substrates During Curing, Postcuring, and Accelerated Degradation

Marcelo Augusto Gonçalves Bardi,[1,2] Mara de Mello Leite Munhoz,[1] Henrique Alves de Oliveira,[1] Rafael Auras,[2] Luci Diva Brocardo Machado[1]

[1]Universidade de São Paulo (USP), Instituto de Pesquisas Energéticas e Nucleares (IPEN/Centro de Tecnologia das Radiações (CTR)), Avenida Professor Lineu Prestes, 2242, Cidade Universitária, São Paulo 05508-000, Brazil

[2]Michigan State University (MSU), School of Packaging, 448 Wilson Road, East Lansing, Michigan 48824

Correspondence to: L. D. B. Machado (E-mail: lmachado@ipen.br)

ABSTRACT: During radiation curing, a reactive formulation is converted into a highly crosslinked coating film by means of polymerization reactions. This three-dimensional (3D) network is resistant to external degrading factors as it cannot be undone by any physical–chemical means. In this study, various ultraviolet (UV)-curable ink formulations with different pigments were developed. The behavior of the UV-curable inks was evaluated during UV curing in a photocalorimeter or in a UV tunnel. Inks were exposed to accelerated aging in an accelerated weathering chamber and their physical–chemical properties were investigated. The presence of residual fractions of unreacted species trapped in the 3D network formed during UV curing interferes with the degradation of the main structure during exposure in the weathering chamber. The ink formulations that did not easily absorb UV light increased in gloss and hardness, indicating that residual crosslinking is taking place at the same time that degradation is occurring. © 2014 Wiley Periodicals, Inc. J. Appl. Polym. Sci. **2014**, *131*, 41116.

KEYWORDS: coatings; crosslinking; degradation; photopolymerization; radical polymerization

Received 23 January 2014; accepted 6 June 2014

DOI: 10.1002/app.41116

INTRODUCTION

During the past few decades, applications of ultraviolet or electron beam (UV/EB) curing technology have increased significantly. According to a survey taken by RadTech North America, around 6×10^4 metric tons of radiation-curable overprint varnish and inks were used by packaging companies between 2010 and 2011.[1] This increase can be partially attributed to regulatory laws regarding the reduction of volatile organic compounds as UV/EB curing process is typically solvent-free.[2–4] Additionally, as the UV/EB polymerization process takes place at room temperature, temperature-sensitive materials, such as paper or thermoplastic polymers, can be easily printed.[3,5]

Radiation curing converts a reactive formulation into a highly crosslinked coating film by an irreversible reaction that provides high chemical resistance and a higher stability against degradation.[6,7] The kinetics of curing depend directly on the formulation composition,[8] and the degradation process of radiation-curable materials requires specific conditions to initiate. Curing is also highly dependent on parameters such as the chemical structure and component of the resins, crosslinking agents, the type and concentration of cure initiators (photoinitiators), and crosslinking parameters in the radiation chamber.[9] High radiation doses during curing can cause degradation of the pigment and affect the whole crosslinked network, as previously reported by the authors.[10] Similarly, Shi et al.[8] determined that moisture is critical for accelerating the degradation of thermal-cured epoxy samples. Accelerated aging chambers, such as QUV (Q-Lab, Westlake, OH) or weather-o-meters, can be used to expose ink samples to simulated aggressive conditions (e.g., UV light, moisture, and corrosive environments), so that the ink properties before and after accelerated aging can be measured.

Pigments also interfere in the curing and degradation processes of epoxy acrylate-based coatings. Moreover, different classes of pigments can have different impacts on curing as they promote either scattering or absorption of UV photons.[10] In general, the degree of curing is reduced when pigments are added to samples cured by UV light.

Besides compositional effects, the substrate can also impact the behavior of epoxy-acrylate materials during curing, or during service periods. For example, barrier properties against water or oxygen are important physical factors for the overall material

substrate protection,[11] and this protection is directly related to the crosslink network density.[9] As discussed by He et al.,[11] an increase in the crosslink density of the cured samples can be expected when samples are exposed to certain degradation environments resulting from initially unreacted fractions of reactive groups in the coating. Chiu et al.[12] compared polycarbonate (PC), poly(vinyl chloride) (PVC), and glass as substrates for UV-curable organic/inorganic hybrid composite coatings, and observed that coated PC films had more light transmittance than PVC or glass, suggesting that the substrate properties must be considered with the overall system.

The aim of this work is to investigate the effect of the pigment composition of UV-curable print inks on two different plastic substrates by evaluating their thermal, optical, and mechanical properties before and after UV accelerated aging. It is observed that the degradation pace is a function of the amount of photons reaching the substrate due to the interaction between pigment particles and UV photons. The substrate can interfere with the degradation reaction depending on its ability on absorbing photons by itself.

EXPERIMENTAL

Materials

The following materials were used to prepare the UV-curable clear coating formulation: bisphenol A epoxy diacrylate resin (EBECRYL® 3720-TP25, Cytec Industries) diluted 25% by weight with tripropylene glycol diacrylate (TPGDA, Cytec Industries); trimethylolpropane triacrylate (TMPTA, Cytec Industries); blend of photoinitiators 4.5/3.5/2.0 1-hydroxycyclohexyl phenyl ketone (Irgacure 184, Ciba-Geigy)/2-hydroxy-2-methyl-1-[4-(1-methylvinyl) phenyl] propanone (Esacure KIP 150, Lamberti)/2-dimethylamino-2-(4-methyl-benzyl)-1-(4-morpholin-4-yl-phenyl)-butan-1-one (Irgacure 379, Ciba Specialty Chemicals); talc (Nicron® 674, Luzenac America); polydimethylsiloxane (Pure Silicone Fluid 100,000cSt, Clearco Products); and polyethylene/polytetrafluoroethylene wax (CeraSPERSE® 164, Shamrock Technology).

To obtain the colored print inks, one of the following pigments was added to the clear coating: carbon black (Printex® 45 powder, Evonik Degussa GmbH); yellow pigment derived from diarylide m-xylidide (Irgalite® Yellow LBIW, Ciba Specialty Chemicals); blue pigment derived from phtalocyanine (Hostaperm Azul B2G 01-BR, Clariant Pigmentos e Aditivos Ltda.); ruby pigment derived from monoazo calcium salts (Rubide 4B, Hongyan Pigment Chemical); and titanium dioxide (Kemira® 660 RDI-S, Kemira Pigments Oy). The ratio of pigment to clear coating was kept constant (21/79, wt/wt) to investigate only the influence of each pigment under UV curing.

Poly(butylene-*co*-adipate terephthalate)/thermoplastic starch (PBAT/TPS) blend sheet (thickness = 1.0 ± 0.0 mm) was kindly supplied by Corn Products do Brasil (Jundiaí, SP, Brazil) and was used as received. Low-density polyethylene (type EB-853/72 and lot RSAB2A096E) pellets were purchased from Braskem S.A. (Camaçari, BA, Brazil). Both materials were used as substrates for the coating formulations described above.

The samples were labeled as (BA, AA)-color-(LDPE, PBAT/TPS), where BA and AA represent "before UV aging" and "after UV aging," respectively, color is the visual color based on the pigment; and LDPE or PBAT/TPS indicates the film substrate, low density polyethylene and poly(butylene-co-adipate terephthalate)/thermoplastic starch respectively. For example, a sample labeled as BA-yellow-LDPE refers to the non-UV aged yellow sample on LDPE film.

LDPE Film Preparation

LDPE film was prepared by blown extrusion in a Lab 16 Chill-roll extruder with an L/D ratio of 26 and a 220-mm wide flat die (AX Plásticos Ltda., Diadema, SP, Brazil). The temperatures used for zones 1, 2, and 3 were 178, 185, and 190°C, respectively, and the screw speed was 80 rpm. The thickness of films were determined with a TMI 549*M* micrometer (Testing Machines, Amityville, NY), and the average measured value for the LDPE film was 21 ± 0.5 μm.

Radiation Curing Procedure

A manual applicator (QuickPeek®, supplied by Boanitec Indústria e Comércio Ltda, Cotia, SP, Brazil) was used to apply the colored print inks on the PBAT/TPS and LDPE. The thickness of the coating ranged from 0.4 to 1.0 μm after curing, depending on the pigment used.

The coating formulations were cured at room temperature by using a Labcure UV tunnel (Germetec UV and IR Technology, Rio de Janeiro, RJ, Brazil). This equipment consisted of a UV medium-pressure mercury lamp (emission wavelength ranging from 300 to 450 nm) and a conveyor belt with adjustable speed. The UV radiation doses were measured with a UV Power Puck radiometer from EIT (Sterling, VA). The coated samples to be cured were placed on the conveyor that moved under UV light beam. The precise control of the conveyor speed determined the radiation dose absorbed by the samples. The power of the lamp was fixed at 118 W cm^{-1}, the conveyor speed was fixed at 0.1 ms^{-1} and the radiation dose was fixed at 550 mJ cm^{-2}.

Specimens of approximately 5 mg of each film sample (coated and uncoated) were placed in a separate aluminum crucible without a lid. Photo-differential scanning calorimetry (photo-DSC) measurements were performed on the specimens with a DSC 6000 (Perkin Elmer, Waltham, MA). A spot UV curing lamp system, model OmniCure® S2000 (Lumen Dynamics, Mississauga, ON, Canada), equipped with a high pressure 200 W mercury vapor short arc (40 mW cm^{-1}) bulb and filtered for 320–500 nm, was attached to the calorimeter. The test was run under isothermal conditions at 30°C and N_2 flow of 50 mL min^{-1}. Figure 1 shows the thermal program used to expose the samples to UV radiation. The cure degree was determined by means of the photo-induced reaction enthalpy, according to eq. (1):

$$P_t = \frac{H_t}{H_\infty} \times 100 \quad (1)$$

where H_t is the reaction enthalpy at t seconds, given in kJ mol^{-1}; and H_∞ is the theoretical value for the reaction heat involved when 100% of the unsaturated acrylic is converted, given as 86 kJ mol^{-1}.[13,14]

The rate of polymerization (R_p) was calculated based on eq. (2):

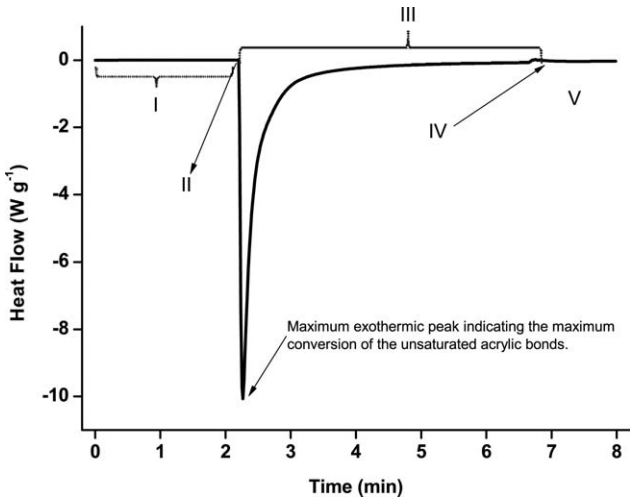

Figure 1. DSC curve from a thermal program involving photopolymerization for the clear coating formulation. Five steps are shown: (I) 2 min for purging and temperature stabilization; (II) opening the obturator; (III) 4.5 min of static exposure to UV radiation; (IV) Closing the obturator; and (V) 1.5 min for stabilization and return to baseline.

$$R_P = \frac{dP}{dt} = \frac{dH/dt}{H_\infty} \quad (2)$$

Measurements for both visible and UV light absorbance (UV-Vis) were performed on a Lambda 25 UV-Vis spectrometer (Perkin-Elmer Instruments, Wellesley, MA). Spectra were acquired at a scanning rate of 480 nm min^{-1}, from 190 to 1100 nm. The extinction coefficient was calculated for the maximum absorbance wavelength (λ_{max}) in the visible wavelength range (400–700 nm) according to the Beer-Lambert law [eq. (3)]:

$$A = \varepsilon l c \quad (3)$$

where A is the measured absorbance (a.u.), ε is the extinction coefficient (cm^{-1}), l is the path length through the sample (cm), and c is the nominal pigment concentration.

Sample Aging

The accelerated aging was performed using an accelerated weathering chamber model EQUV (Equilam Ind. e Com. Ltda., Diadema, SP, Brazil) following ASTM D5208-09, cycle C. A fluorescent bulb, UVB with 0.89 W m^{-2} nm^{-1} irradiance (at 340 nm), was used with cycles of UV radiation under a UV-incident beam at 90° and constant temperature at 50 ± 3°C. The samples were subjected to the aging process for 250 h nonstop.

Characterization

Aged and nonaged samples were evaluated by means of the following experiments:

Color and gloss measurements were performed with a Spectro-Guide Sphere Gloss portable spectrophotometer (Byk-Gardner GmbH, Geretsried, Germany). A D65/10° geometry was used, and data from three different positions of the samples were collected. The L*a*b* coordinates and gloss index are reported.

König film hardness as reported in seconds was evaluated according to ISO 1522 : 2006(E) using a pendulum hardness tester (Byk-Gardner GmbH). To measure the hardness properly, the glass plate used for the König pendulum calibration was used as a rigid substrate for the polymeric films during the runs; similar methodology has been published previously.[10]

Fourier-transformed infrared (FTIR) spectra were collected using an FTIR spectrophotometer, model IRPrestige-21 (Shimadzu, Kyoto, Japan), equipped with an attenuated total reflectance (ATR) attachment (PIKE Technologies, Madison, WI); spectra were collected from 4000 to 650 cm^{-1}. The polymerization and residual polymerization were followed by the changes on the IR band at 1635 cm^{-1} of the acrylate double bond.[15] The values were normalized based on the absorbance at 1730 cm^{-1} related to the C═O stretching vibration of the acrylate monomers, which was practically constant for all the formulations.

RESULTS AND DISCUSSION

Figures 2(a–c) show the heat flow curves, the photo-conversion curves and the photopolymerization rate curves, respectively, as a function of time, for the inks exposed to UV radiation in the photocalorimeter. The effect of the pigments on the curing process is depicted by the overall reduction of the exothermic heat flow peaks compared with that of the clear coating [Figure 2(a)]. For the photopolymerizable epoxy acrylate clear coating samples, in general, the higher the concentration of acrylic groups per mol, the lower the maximum reaction heat flow, possibly due to an entanglement of the epoxy acrylate oligomers when a rapid increase in molecular weight takes place.[16,17] The maximum exothermic heat flow observed in this work ($h = 16.9$ W g^{-1}) is in accordance with similar values obtained by Park et al.[16] This mechanism can also be correlated with the polymerization rate values [Figure 2(c)], which reach a maximum of 35.2 × 10^{-4} s^{-1} at 8.0 s and then decrease to 17.7 × 10^{-4}, 7.1 × 10^{-4}, and 3.8 × 10^{-4} s^{-1} at 16.0, 24.0, and 32.0 s, respectively, and with the corresponding acrylate conversions [Figure 2(b)] of 2.2, 24.3, 32.8, and 36.7%, respectively.

Additionally, the exothermic peak height tends to be correlated with the concentration of free radicals that increases the exothermic reaction energy. The observed reduction is directly associated with the different interactions that may happen between light and the pigments,[18] and is generally associated with a reduced absorption of photons by the reactive species of the photoinitiator. For instance, samples containing black pigment (carbon black) had the lowest heat flow values [Figure 2(a)]. Carbon black is a light-shielding material and a free radical scavenger, so the light absorbed by the photoinitiator would be reduced and the radical produced by the photoinitiator will be easily trapped or deactivated by the pigment.[19–21] Similar values for the polymerization rates (around 3.0 × 10^{-4} s^{-1}) observed in this work were reported by Kuo et al.[20] The behavior of the yellow-pigmented samples was similar to that of the black-pigmented samples during photo-DSC tests (Figure 2). According to Vasilakos and Tarantili,[18] the low values for heat flow of the yellow samples are due to the great interaction between UV light and the yellow chromaticity.

The interaction of the incident radiation with the different ink formulations is depicted in Figure 3(a). The spectra for the

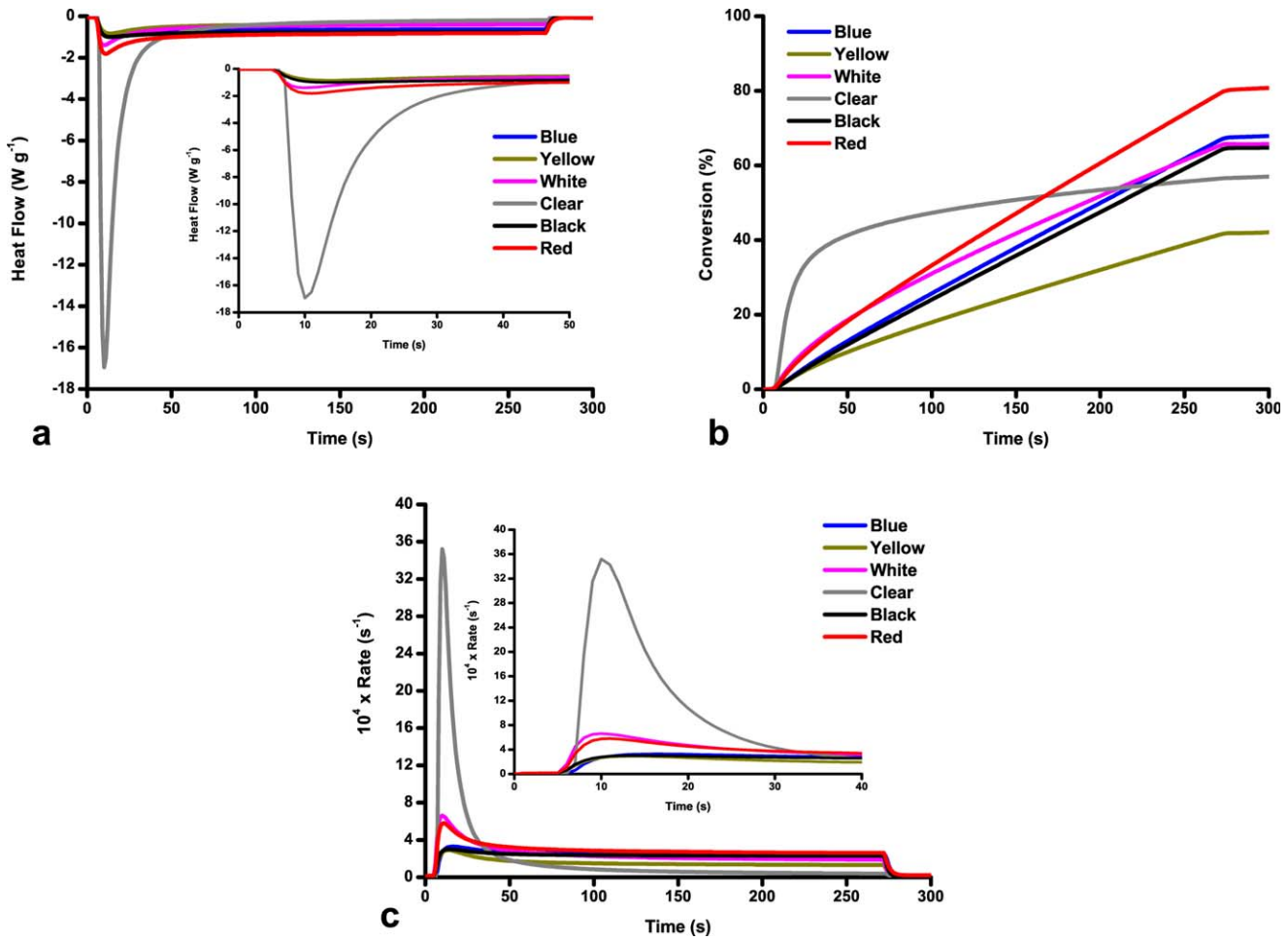

Figure 2. Thermal behavior from UV-induced crosslinking reactions in a DSC coupled with a UV light source for inks containing different pigments: (a) heat flow curves, (b) photo-conversion curves, and (c) reaction rate curves. [Color figure can be viewed in the online issue, which is available at wileyonlinelibrary.com.]

cured samples coated over LDPE show that the substrate is totally transparent to the radiation at the tested wavelength range. The same behavior is observed for the clear coating formulation. This suggests that the resin, the monomer and the photoinitiator do not interact with radiation after curing in the UV range. Table I shows the values for λ_{max} and the extinction coefficient (ε_{max}) for the analyzed LDPE-coated samples.

The black ink had constant absorption throughout the visible wavelength range. The white ink had similar behavior in the 400–550 nm range, but presented a lower extinction coefficient than the black ink. The relatively lower ε_{max} represents the tendency of the white ink to reflect more photons from the visible part of the electromagnetic spectra, reducing the color strength.

As expected, the other colors studied present very well-defined absorbance bands for the visible wavelengths, with half-widths around 40 nm each. For the blue ink, the bands are centered at 634 and 714 nm, for the red ink at 405 and 576 nm, and for the yellow ink at 441 nm. The ε_{max} values are very similar for the black, blue, and red ink compositions, but a hypochromic tendency for the yellow ink composition was observed as the absorption values shift to lower wavelengths. These absorbance regions basically depend on the chromophoric group in each pigment. Absorbance is depicted graphically in Figure 4.

The absorbance of all the ink compositions tended to increase substantially in the far-UV region (below 250 nm). In the 300–400 nm range, absorbance bands with half-widths around 40 nm for blue (centered at 338 nm) and red (at 328 nm) were observed. The absorbance region for the photoinitiator blend is in this wavelength range. The relatively higher curing degree for these samples can be explained by an energy transfer mechanism from the chromophoric groups of the pigments to the photoinitiatior molecules, which increases the crosslinking ratio. Also, the lack of an absorbance peak for the 320–400 range is due to the low degree of curing for the yellow ink composition.

Similar analyses can be drawn by numerically integrating the absorbance values under the absorbance curves in the range of 300–400 nm. As shown in Figure 4, the total absorbance is 35% higher for the red ink than for the yellow ink. This finding corroborates that red ink must have a relative higher curing degree than the yellow ink, as the former can absorb much more photons on the studied wavelength than the latter.

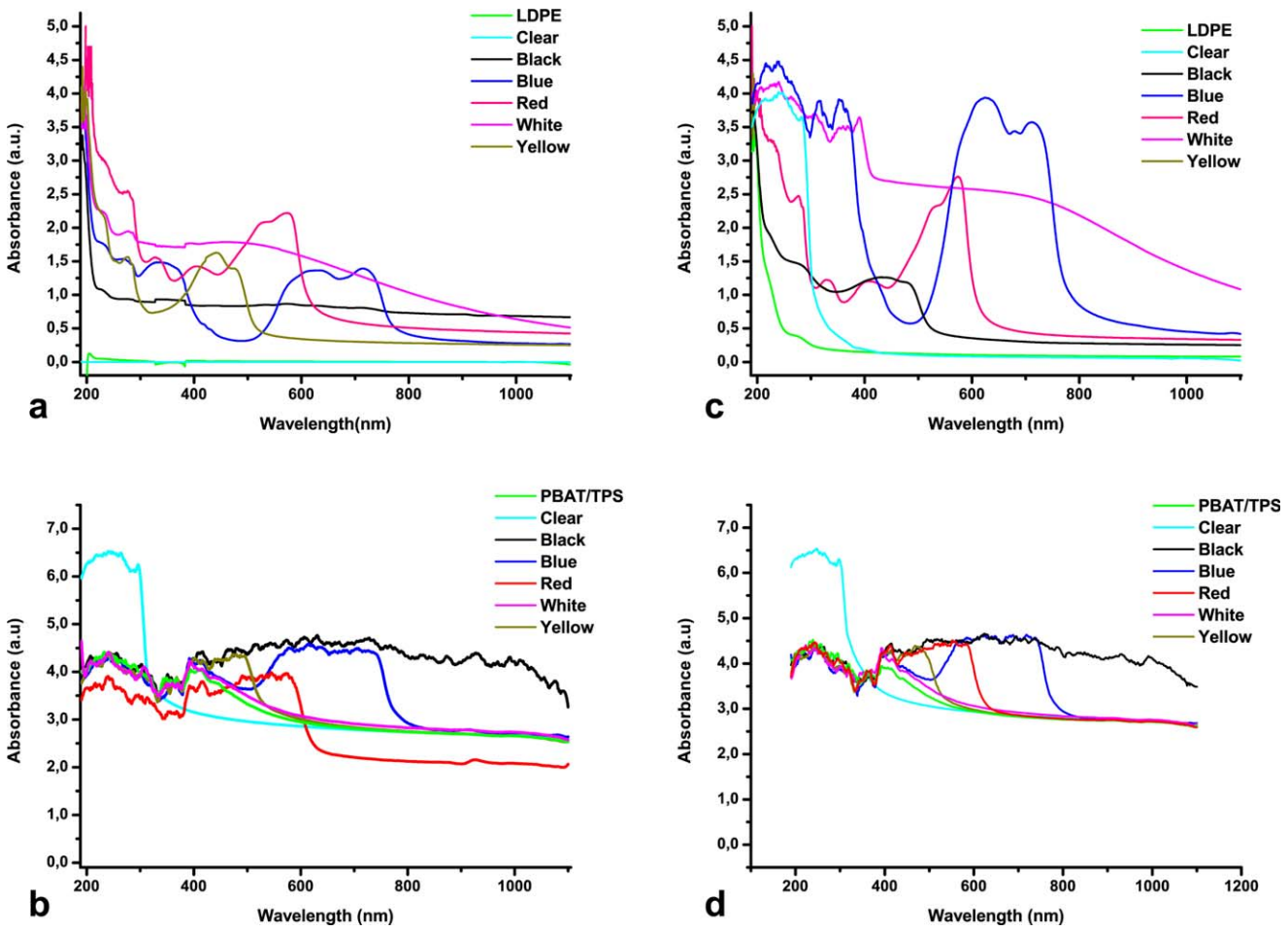

Figure 3. Absorbance spectra for (a) BA-LDPE and BA-color-LDPE, (b) BA-PBAT/TPS and BA-color-PBAT/TPS, (c) AA-LDPE and AA-color-LDPE, and (d) AA-PBAT/TPS and AA-color-PBAT/TPS. [Color figure can be viewed in the online issue, which is available at wileyonlinelibrary.com.]

Figure 5 shows the resulting FTIR-ATR absorption ratios (A1635/A1730) where 1635 cm^{-1} corresponds to the —C═C— absorbance band for (BA, AA)-LDPE, (BA, AA)-color-LDPE, (BA, AA)-PBAT/TPS, and (BA, AA)-color-PBAT/TPS.

During the accelerated UV aging, samples are exposed to UV radiation for a much longer time (i.e., 250 h in the QUV chamber) than during UV curing (<5 s, depending on the conveyor speed in the UV tunnel), so then some of the trapped reactive species can undergo random recombination in the crosslinking. This process, called residual curing, could be observed by the similar ratios (Figure 5) for the AA-blue-LDPE compared with the BA-blue-LDPE, and AA-clear-LDPE compared with BA-clear-LDPE.

Interestingly, other ink formulations showed an increase in the double bond content, in this study, after the aging in the QUV chamber. This increase can be associated with photoinduced

Table I. UV and Visible Absorbance Parameters Obtained for (BA, AA)-(LDPE, PBAT/TPS) Films and (BA, AA)-Color-(LDPE or PBAT/TPS) Coated Films

	LDPE					PBAT-TPS				
	Black	Blue	Red	White	Yellow	Black	Blue	Red	White	Yellow
BA-λ_{max} (nm)	573	634	576	455	441	463	577	551	401	402
AA-λ_{max} (nm)	569	619	574	400	430	496	649	520	403	470
BA-$\alpha_{\lambda_{max}}$ ($\times 10^4$ cm^{-1})	2.4	2.6	2.6	1.2	3.1	0.0	0.0	0.0	0.0	0.0
AA-$\alpha_{\lambda_{max}}$ ($\times 10^4$ cm^{-1})	8.2	7.4	3.3	2.2	2.4	0.0	0.0	0.0	0.0	0.0
BA-$\alpha_{\lambda_{313}}$ ($\times 10^4$ cm^{-1})	2.4	2.6	1.8	1.2	1.4	0.0	0.0	0.0	0.0	0.0
AA-$\alpha_{\lambda_{313}}$ ($\times 10^4$ cm^{-1})	8.8	6.7	1.3	2.5	2.2	0.0	0.0	0.0	0.0	0.0
Fade (%)	−246.5	−187.3	−24.3	2.3	22.7	14.0	3.7	3.7	1.8	18.1

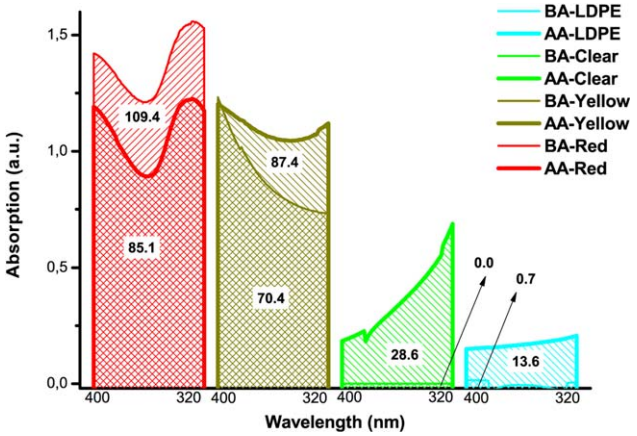

Figure 4. Area under the absorbance curve for (BA, AA)-LDPE, (BA, AA)-clear-LDPE, (BA, AA)-red-LDPE, and (BA, AA)-yellow-LDPE for wavelengths in the 320–400 nm range. [Color figure can be viewed in the online issue, which is available at wileyonlinelibrary.com.]

degradation of the polymeric substrate and the further migration of its by-products to the surface of the polymeric film.

The UV exposure of PBAT/TPS film during accelerated aging has not caused meaningful alterations in the A1635/A1730 FTIR-ATR absorbance ratio, as reported by Chen et al.[22] Nevertheless, the TPS phase can be greatly affected by the abiotic degradation step,[23,24] resulting in chain scission and radical generation on the glucosidic ring, producing starch dialdehyde and then followed by the production of formaldehyde, formic acid and CO_2.

The abiotic degradation of LDPE by UV light has been studied and reported elsewhere.[25–27] In general, photo-oxidation increases both the amount of low molecular weight material, during chemical bond breakage, and the surface area, by embrittlement.[26] According to Albertsson et al.[26] and Amin et al.,[27] one of the steps of the abiotic degradation of polyethylene refers to the formation of double bonded by-products due to the Norrish II reaction, which can be followed by the IR double bond index (absorbance at 1635 cm^{-1}, A1635). In this study, the

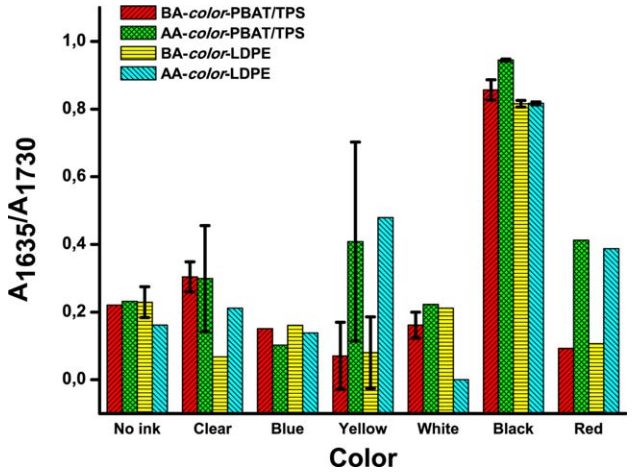

Figure 5. Normalized average values of IR absorbance at 1635 cm^{-1}/1730 cm^{-1} for (BA, AA)-PBAT/TPS, (BA, AA)-LDPE, (BA, AA)-color-PBAT/TPS, and (BA, AA)-color-LDPE. [Color figure can be viewed in the online issue, which is available at wileyonlinelibrary.com.]

double bond concentration increased over time for the AA-LDPE films at 250 h of UV exposure, with a final $A1635_{AA\text{-}LDPE}/A1635_{BA\text{-}LDPE}$ ratio of 5.6. This value is in agreement with the UV-aging of uncoated polyethylene for up to 1500 h, which was previously calculated to be 6.4.[26]

The coating of LDPE with yellow ink caused a reduction in the carbon–carbon double bond IR absorbance band, as was expected for the yellow sample. Again, this result is due to the competitive mechanisms of residual curing and photodegradation. The cured coating appears to be capable of protecting the polyolefin from photodegradation, and part of this energy is then used for the residual curing. This process is dependent on the pigment and on the degree of curing of each coating, as was discussed above.

Table II presents the average values, and their respective standard deviation, for L*a*b* indexes, gloss, and hardness for (BA, AA)-(LDPE, PBAT/TPS) films and (BA, AA)-color-(LDPE, PBAT/TPS) coated films to show the impact of different degrees of curing on some physical properties.

The measurement of the color indices $L^*a^*b^*$ is very useful to complement the curing analyses performed by photo-DSC and ATR-FTIR. The component L^* represents the lightness and its magnitude varies from 100 (light) to 0 (dark), whereas a^* and b^* components are the chromaticity indices where $+a^*$ is for reddish, $-a^*$ for greenish, $+b^*$ for yellowish, and $-b^*$ for bluish color indications.[28]

The L^* index for (BA, AA)-color-(PBAT/TPS, LDPE) was greatly affected by the lightness of the substrate. LDPE films had a higher average L^* than did PBAT/TPS films, although this difference was reduced after UV irradiation, as shown by the increase in the average L^* value in AA-PBAT/TPS compared with BA-PBAT/TPS. This trend could also be observed for the samples (BA, AA)-clear-(PBAT/TPS, LDPE), (BA, AA)-white-(PBAT/TPS, LDPE), and (BA, AA)-yellow-(PBAT/TPS, LDPE). However, the same behavior was not observed for the a^* and b^* indices. There was no obvious relationship between a^* and b^* indices and the film substrate used, which seems to indicate that these properties are purely dependent on the pigment incorporated in the ink. An exception to this rule is the clear formulation, which does not contain any pigment. During the curing process, the reaction rate for the clear formulation is very high, but the resulting curing degree is relatively low, as can be seen in Figure 2(c). So, during the aging process, UV photons have a free path to interact with the substrate as well, giving rise to the degradation of both the coating layer and substrate.

A significant increase in a^* and b^* for AA-yellow-(PBAT/TPS, LDPE) was observed independently of the substrate. According to a previous publication by the authors,[10] the yellow pigment is very sensitive to UV radiation. The increase in the b^* index can be related to the excellent light fastness properties of the yellow pigment,[29] once UV photons interact positively with the chromophoric diarylide group in the pigment structure, although the pigment particles are susceptible to long-term weathering degradation.[30]

The gloss index is generally an indicator for the quality of the curing process. UV-radiation curable print inks have a higher

Table II. Optical and Mechanical Properties for (BA, AA)-(LDPE, PBAT/TPS) Films and (BA, AA)-Color-(LDPE, PBAT/TPS) Coated Films

Film sample	L*	a*	b*	Gloss	Hardness (s)
BA-PBAT/TPS	80.1 ± 0.2^{a}	3.7 ± 0.1^{a}	16.4 ± 0.1^{a}	27.6 ± 5.0^{a}	47.7 ± 2.1^{a}
AA-PBAT/TPS	84.5 ± 0.4^{b}	1.3 ± 0.1^{b}	10.7 ± 0.4^{b}	47.0 ± 2.5^{a}	63.0 ± 1.7^{b}
BA-LDPE	89.4 ± 0.3^{c}	0.2 ± 0.0^{c}	2.0 ± 0.1^{c}	91.5 ± 22.3^{b}	31.0 ± 1.0^{c}
AA-LDPE	89.2 ± 0.1^{c}	0.2 ± 0.0^{c}	2.2 ± 0.0^{c}	79.4 ± 4.0^{b}	32.0 ± 0.0^{c}
BA-Clear-PBAT/TPS	80.7 ± 0.2^{a}	-0.7 ± 0.0^{a}	5.2 ± 0.1^{a}	77.2 ± 13.6^{a}	50.0 ± 3.0^{a}
AA-Clear-PBAT/TPS	89.3 ± 1.0^{b}	-0.8 ± 0.1^{a}	13.4 ± 2.9^{b}	45.6 ± 38.6^{a}	59.3 ± 2.1^{b}
BA-Clear-LDPE	80.2 ± 0.3^{a}	-0.4 ± 0.0^{b}	5.7 ± 0.0^{a}	72.7 ± 40.4^{a}	35.3 ± 2.1^{c}
AA-Clear-LDPE	90.5 ± 0.2^{b}	-0.7 ± 0.1^{a}	7.4 ± 1.0^{a}	80.6 ± 18.8^{a}	33.7 ± 1.1^{c}
BA-Red-PBAT/TPS	39.9 ± 0.4^{a}	41.3 ± 0.3^{a}	21.9 ± 0.4^{a}	18.6 ± 1.6^{ab}	45.7 ± 2.5^{a}
AA-Red-PBAT/TPS	38.1 ± 0.6^{b}	38.4 ± 0.9^{b}	20.5 ± 0.8^{bc}	18.3 ± 2.3^{ab}	47.7 ± 0.6^{a}
BA-Red-LDPE	41.4 ± 0.3^{c}	44.5 ± 0.5^{c}	21.2 ± 0.4^{ab}	17.1 ± 1.9^{b}	33.3 ± 1.5^{b}
AA-Red-LDPE	39.7 ± 0.2^{a}	40.1 ± 0.2^{a}	19.5 ± 0.3^{c}	23.7 ± 2.9^{a}	33.7 ± 1.5^{b}
BA-Blue-PBAT/TPS	33.5 ± 0.3^{a}	-3.5 ± 0.3^{a}	-29.3 ± 0.3^{a}	24.7 ± 1.9^{a}	50.7 ± 0.6^{a}
AA-Blue-PBAT/TPS	33.9 ± 0.5^{a}	-3.7 ± 0.7^{a}	-31.2 ± 0.3^{b}	45.1 ± 1.5^{b}	67.0 ± 6.0^{b}
BA-Blue-LDPE	42.1 ± 0.7^{b}	-14.6 ± 0.4^{b}	-39.9 ± 0.2^{c}	8.1 ± 1.1^{c}	$32.\ 7 \pm 0.6^{c}$
AA-Blue-LDPE	41.9 ± 0.3^{b}	-14.1 ± 0.8^{b}	-39.5 ± 0.1^{c}	20.7 ± 7.9^{a}	29.0 ± 3.0^{c}
BA-Black-PBAT/TPS	25.4 ± 0.1^{a}	2.1 ± 0.0^{a}	-0.5 ± 0.1^{a}	46.1 ± 15.5^{a}	51.7 ± 1.5^{a}
AA-Black-PBAT/TPS	25.0 ± 0.4^{a}	1.9 ± 0.1^{ab}	-0.5 ± 0.2^{a}	41.2 ± 2.4^{a}	53.0 ± 2.0^{a}
BA-Black-LDPE	25.4 ± 0.2^{a}	1.8 ± 0.1^{b}	-1.1 ± 0.2^{b}	9.2 ± 0.2^{b}	31.0 ± 1.0^{b}
AA-Black-LDPE	26.3 ± 0.2^{b}	2.0 ± 0.1^{ab}	0.4 ± 0.0^{c}	15.0 ± 3.4^{b}	32.0 ± 2.6^{b}
BA-White-PBAT/TPS	86.9 ± 0.7^{a}	1.9 ± 0.5^{a}	4.8 ± 0.5^{a}	39.7 ± 2.3^{a}	51.3 ± 0.6^{a}
AA-White-PBAT/TPS	88.2 ± 0.2^{a}	0.8 ± 0.1^{b}	5.1 ± 0.1^{a}	51.4 ± 3.5^{ab}	56.7 ± 2.3^{b}
BA-White-LDPE	90.2 ± 1.2^{b}	-0.5 ± 0.1^{c}	1.2 ± 0.1^{b}	26.0 ± 4.7^{c}	34.0 ± 1.7^{c}
AA-White-LDPE	91.3 ± 0.1^{b}	-0.8 ± 0.1^{c}	3.4 ± 0.3^{c}	60.0 ± 7.2^{b}	33.3 ± 1.5^{c}
BA-Yellow-PBAT/TPS	74.6 ± 0.3^{a}	10.8 ± 0.2^{a}	72.9 ± 0.4^{a}	32.0 ± 2.9^{a}	50.7 ± 0.6^{a}
AA-Yellow-PBAT/TPS	75.6 ± 0.1^{b}	12.1 ± 0.2^{b}	79.1 ± 0.8^{b}	37.9 ± 2.8^{b}	62.7 ± 1.5^{b}
BA-Yellow-LDPE	80.0 ± 0.2^{c}	7.2 ± 0.1^{c}	81.8 ± 1.2^{bc}	35.1 ± 1.3^{ab}	32.7 ± 0.6^{c}
AA-Yellow-LDPE	78.1 ± 0.2^{d}	10.2 ± 0.5^{a}	85.6 ± 3.6^{c}	24.1 ± 1.1^{c}	30.7 ± 2.3^{c}

Note: Values are given as means ± SD. Values in the same column for the same color (i.e., clear, red, etc.,), with same lower superscript letters are not significantly different at type I error (α) of 0.05, using the Tukey-Kramer test.

gloss level than traditional solvent-based formulations.[10] The increase in gloss after radiation treatment indicates that crosslinking reactions induced by UV photons were taking place, whereas a decrease indicates that the structure is being damaged by the photodegradation process. Samples with lower degrees of curing, such as the black and blue ink compositions, had the highest increase in gloss values after UV aging. However, a numerical correlation between curing degree and gloss index was not strictly observed, as residual curing during aging competes against the abiotic degradation process.

Similar conclusions can be drawn from the König hardness average values (Table II), which are a valuable indication of curing and degradation processes. However, König hardness values seem greatly dependent on the substrate surface, and can also indicate degradation of the polymeric film below the very thin coating layer. In this study, there was no relationship between the numerical values of curing degree and hardness.

The UV-VIS absorbance spectra were also affected by the UV aging process, as shown in Figure 3(c) and compared with Figure 3(a). Blue, black, red, and white samples had hyperchromic shifts in the visible wavelength region, as summarized by the values of λ_{max} in Table I. Yellow samples had hypochromic shifts. This reduction in color strength for the yellow formulation may indicate the predominance of degradation of the pigment on the overall photoreactions in the sample. The inorganic pigments, that is titanium dioxide, the phthalocyanin-based blue pigment and the monoazo red in LDPE compositions showed considerable high light-fastness, as suggested by the low fade values in Table I. The diarylide yellow pigment showed a similar level of fade on both polymeric substrates. These alterations in fade (%) were also apparent when the area under the absorbance curve was calculated, as shown in Figure 4.

Lastly, it is important to note the change in the extinction coefficient for the pigmented compositions at 340 nm, the wavelength used during the QUV accelerated degradation test (Table I). AA-red-LDPE was the only sample in which the a^* value was slightly reduced after the radiation treatment, either due to residual crosslinking or the photo-oxidation process.

CONCLUSIONS

UV-curable inks were coated into LDPE and PBAT/TPS samples. The behavior of the UV-curable inks was evaluated using a photocalorimeter and a UV-tunnel. No meaningful variations in the color and gloss properties were observed for the different substrates when the UV-cured ink films were exposed to accelerated aging in a QUV chamber for 250 h. However, greater fading was observed for the coatings applied on PBAT/TPS than on LDPE. The curing degree of each photocurable composition was a key factor during the UV aging due to the number of unreacted species trapped in the crosslinked network as well as to the kind of interaction between the pigments and the UV photons (scattering or absorption). Further work should be conducted to unveil the mechanism of interaction between the ink formulation and the substrate.

ACKNOWLEDGMENTS

The authors thank Fundação de Amparo à Pesquisa do Estado de São Paulo—FAPESP for financial support (grant n. 2010/02631-0), and Conselho Nacional de Desenvolvimento Científico e Tecnológico—CNPq for scholarships. The authors also thank Flint Ink do Brasil S.A. (Cotia, SP, Brazil) for opening their laboratory infrastructure for preparing the print inks, and Dr. Isolda Costa for the use of QUV facility.

REFERENCES

1. Cohen, G. *RadTech. Report* **2012**, *5*, 44.
2. Salleh, N. G. N.; Yhaya, M. F.; Hassan, A.; Bakar, A. A.; Mokhtar, M. *Radiat. Phys. Chem.* **2011**, *80*, 136.
3. Bauer, F.; Decker, U.; Czihal, K.; Mehnert, R.; Riedel, C.; Riemschneider, M.; Schubert, R.; Buchmeiser, M. R. *Prog. Org. Coat.* **2009**, *64*, 474.
4. Chen, Z.; Wu, J. F.; Fernando, S.; Jagodzinski, K. *Prog. Org. Coat.* **2011**, *71*, 98.
5. Salleh, N. G. N.; Alias, M. S.; Gläsel, H.-J.; Mehnert, R. *Radiat. Phys. Chem.* **2011**, *80*, 136.
6. Chen, L.; Zhou, S.; Song, S.; Zhang, B.; Gu, G. *J. Coat. Technol. Res.* **2011**, *8*, 481.
7. Shi, X.; Hinderliter, B. R.; Croll, S. G. *J. Coat. Technol. Res.* **2010**, *7*, 419.
8. Mishra, R. S.; Mishra, A. K.; Raju, K. V. S. N. *Eur. Polym. J.* **2009**, *45*, 960.
9. Tang, C.; Liu, W. *J. Appl. Polym. Sci.* **2010**, *117*, 1859.
10. Bardi, M. A. G.; Machado, L. D. B. *Radiat. Phys. Chem.* **2012**, *81*, 1332.
11. He, J.; Chisholm, B. J.; Mayo, B. A.; Bao, H.; Risan J.; Christianson, D. A.; Rafferty, C. L. *J. Coat. Technol. Res.* **2012**, *9*, 423.
12. Chiu, H. -T.; Chang, C. -Y.; Chen, C. -L.; Chiang, T. -Y.; Guo, M. -T. *J. Appl. Polym. Sci.* **2011**, *120*, 202.
13. Hu, L.; Asif, A.; Xie, J.; Shi, W. *Polym. Adv. Technol.* **2011**, *22*, 1673.
14. Doğruyol, Z.; Arsu, N.; Doğruyol, S. K.; Pekcan, Ö. *Prog. Org. Coat.* **2012**, *74*, 181.
15. Landry, V.; Riedl, B.; Blanchet, P. *Prog. Org. Coat.* **2008**, *62*, 400.
16. Park, Y. -J.; Lim, D. -H.; Kim, H. -J.; Park, D. -S.; Sung, I. -K. *Int. J. Adhes. Adhes.* **2009**, *29*, 710.
17. Lee, S. -W.; Park, J. -W.; Park, C. -H.; Lim, D. -H.; Kim, H. -J.; Song, J. -Y.; Lee, J. -H. *Int. J. Adhes. Adhes.* **2013**, *44*, 138.
18. Vasilakos, S. P.; Tarantili, P. A. *J. Appl. Polym. Sci.* **2010**, *118*, 2659.
19. Kuo, K. -H.; Chiu, W. -Y.; Don, T. -M. *J. Appl. Polym. Sci.* **2010**, *115*, 1803.
20. Kuo, K. -H.; Chiu, W. -Y.; Hsieh, K. -H.; Don, T. -M. *Eur. Polym. J.* **2009**, *45*, 474.
21. Kuo, K. -H.; Peng, Y. -H.; Chiu, W. -Y.; Don, T. -M. *J. Polym. Sci. Part A* **2008**, *46*, 6185.
22. Chen, J. -H.; Chen, C. -C.; Yang, M. -C. *J. Polym. Res.* **2011**, *18*, 2151.
23. Raquez, J. -M.; Bourgeois, A.; Jacobs, H.; Dégee, P.; Alexandre, M.; Dubois, P. *J. Appl. Polym. Sci.* **2011**, *122*, 489.
24. Campos, A.; Marconcini, J. M.; Martins-Franchetti, S. M.; Mattoso, L. H. C. *Polym. Degrad. Stab.* **2012**, *97*, 1948.
25. Russo, P.; Acierno, D.; Marinucci, L.; Greco, A.; Frigione, M. *J. Appl. Polym. Sci.* **2013**, *217*, 2213.
26. Albertsson, A. -C.; Andersson, S. O.; Karlsson, S. *Polym. Degrad. Stab.* **1987**, *18*, 73.
27. Amin, M. U.; Scott, G.; Tillekeratne, L. M. K. *Eur. Polym. J.* **1975**, *11*, 85.
28. Saha, S.; Kocaefe, D.; Boluk, Y.; Pichette, A. *Prog. Org. Coat.* **2001**, *70*, 376.
29. Colombini, A.; Kaifas, D. e-PS 2010, 7, 14.
30. Mathew, W. R.; Grossman, R. F. In Colorants for Vinyl, Grossman, R. F., Ed.; Handbook of Vinyl Formulating, 2nd ed.; Wiley: Hoboken, **2008**, p 135.